HHS Public Access

Author manuscript

Mech Ageing Dev. Author manuscript; available in PMC 2018 June 22.

Published in final edited form as:

Mech Ageing Dev. 2018 April ; 171: 24–30. doi:10.1016/j.mad.2018.03.001.

Tropomyosin 2 heterozygous knockout in mice using CRISPR-Cas9 system displays the inhibition of injury-induced epithelial-mesenchymal transition, and lens opacity

Teppei Shibata[a], **Shinsuke Shibata**[a], **Yasuhito Ishigaki**[c], **Etsuko Kiyokawa**[b], **Masahito Ikawa**[d], **Dhirendra P. Singh**[e], **Hiroshi Sasaki**[a], and **Eri Kubo**[a,*]

[a]Department of Ophthalmology, Kanazawa Medical University, Ishikawa, Japan

[b]Department of Oncogenic Pathology, Kanazawa Medical University, Ishikawa, Japan

[c]Medical Research Institute, Kanazawa Medical University, Ishikawa, Japan

[d]Research Institute for Microbial Diseases, Osaka University, Osaka, Japan

[e]Department of Ophthalmology and Visual Sciences, University of Nebraska Medical Center, Omaha, NE, USA

Abstract

The process of epithelial–mesenchymal transition (EMT) of lens epithelial cells (LECs) after cataract surgery contributes to tissue fibrosis, wound healing and lens regeneration *via* a mechanism not yet fully understood. Here, we show that tropomyosin 2 (Tpm2) plays a critical role in wound healing and lens aging. Posterior capsular opacification (PCO) after lens extraction surgery was accompanied by elevated expression of *Tpm2*. Tpm2 heterozygous knockout mice, generated *via* the clustered regularly interspaced short palindromic repeat/ Cas9 (CRISPR/Cas9) system showed promoted progression of cataract with age. Further, injury-induced EMT of the mouse lens epithelium, as evaluated histologically and by the expression patterns of *Tpm1* and *Tpm2*, was attenuated in the absence of *Tpm2*. In conclusion, Tpm2 may be important in maintaining lens physiology and morphology. However, Tpm2 is involved in the progression of EMT during the wound healing process of mouse LECs, suggesting that inhibition of *Tpm2* may suppress PCO.

Keywords

Tropomyosin; Lens; Posterior capsular opacification; Epithelial-mesenchymal transition; Cataract

*Corresponding author at: Department of Ophthalmology, Kanazawa Medical University, 1-1 Daigaku, Kahoku, Ishikawa 920-0293, Japan. kuboe@kanazawa-med.ac.jp (E. Kubo).

Conflict of interest statement

This study was partly funded by Ono Pharmaceutical Co. Ltd (Osaka Japan) (to Eri Kubo).

1. Introduction

The epithelial to mesenchymal transition (EMT) is a fundamental process contributing to normal embryonic development, as well as to wound healing and tissue fibrosis (Thiery, 2003). EMT has been reported to be a major factor in the progression of several diseases, including cataract (de Iongh et al., 2005; Rungger-Brandle et al., 2005). Age-related cataract, the leading cause of blindness worldwide, is treated by surgical intervention. However, cell growth across the lens capsule following cataract surgery often leads to fibrosis and secondary visual loss, known as posterior capsular opacification (PCO), secondary cataracts or after-cataracts (McDonnell et al., 1985; Wormstone, 2002). Advances in surgical techniques, and intraocular lens materials and designs have reduced the PCO rate, but it remains a significant problem, especially in young and infant patients (Apple et al., 1992; Awasthi et al., 2009).

EMT of lens epithelial cells (LECs) is regarded as a major cause of PCO after cataract surgery (Lovicu and McAvoy, 1989; Marcantonio et al., 2003; Saika, 2004; Wormstone, 2002). At present, PCO is treated by neodymium-doped yttrium aluminum garnet (Nd:YAG) laser capsulotomy, which is associated with a small risk of sight-threatening complications, such as cystoid macular edema and retinal detachment, and is expensive (Meacock et al., 2000). Nd-YAG laser capsulotomy is frequently unavailable in underdeveloped countries, adding considerably to the problems of treating cataract-associated blindness in third-world settings. The clinical and economic significance of PCO makes it an important public health problem, with prevention of PCO requiring a clear understanding of its pathogenesis (Meacock et al., 2000).

We previously reported that expressions of the high molecular weight tropomyosin (Tpm), isoforms Tpm1 and Tpm2, encoded by the *Tpm1* and *Tpm2* genes, respectively, were elevated in a rodent model of PCO and in LECs obtained from cataractous human patients of various ages (Kubo et al., 2013). The levels of expression of Tpm1and Tpm2, which were found to be minimal in rat LECs, were shown to be increased during EMT, with these increases correlating with fibrosis observed in rat PCO (Kubo et al., 2013). Other cellular abnormalities, particularly the aberrant expression of cytoskeletal and extracellular matrix proteins, were found to be induced by the upregulation of cellular signaling mediated by reactive oxygen species (ROS) (Liu and Gaston Pravia, 2010). Specifically, ROS upregulates transforming growth factor (TGF) β1-mediated signaling (Fatma et al., 2008; Fatma et al., 2005), resulting in the aberrant expression of certain genes, including those encoding α-smooth muscle actin (SMA) and TGFβ-inducible gene-h3 (βig-h3) which are involved in the induction of cataracts and PCO as well as other pathophysiological disorders of cells and tissues (Fatma et al., 2005; McAvoy et al., 2000; Tripathi et al., 1991).

We also previously reported that LECs deficient in peroxiredoxin 6 (Prdx6) showed phenotypic changes, a characteristic of terminal cell differentiation and EMT (Fatma et al., 2005). Prdx6 provides cytoprotection against internal and external environmental stresses and plays a role in cellular signaling by detoxifying ROS, thereby controlling gene regulation (Fatma et al., 2005; Kubo et al., 2008; Manevich and Fisher, 2005; Wood et al., 2003). Proteomic analysis showed that expression of the cytoskeletal proteins Tpm1, Tpm2,

and vimentin was elevated in Prdx6-deficient (*Prdx6*$^{-/-}$) mouse LECs (MLECs) (Kubo et al., 2010). Importantly, the addition of exogenous Prdx6 reduced Tpm2 expression. The involvement of Tpms in the regulation of cellular activities, by stabilizing extracellular matrix (ECM) proteins (specifically actin microfilaments), suggested that aberrant expression of *Tpm1* and *Tpm2* genes is likely involved in the phenotypic alterations observed in *Prdx6*$^{-/-}$ MLECs.

Functionally, Tpms are proteins that stabilize F-actin filaments, regulating the dynamic and structural properties of these filaments by controlling their interactions with actin binding proteins (Gunning et al., 2008; Gunning et al., 2005; Schevzov et al., 2011). For consistency, the human *Tpm* genes should be known as *Tpm1* through *Tpm4*, corresponding to *Tpm1* through *Tpm4* in mice and rats (Geeves et al., 2015). Alternative exon splicing of the *Tpm* genes (Schevzov et al., 2011) can produce up to 40 different mRNA variants, most of which are expressed as protein isoforms in different tissues (Schevzov et al., 2011; Vindin and Gunning, 2013). The balances among levels of isoforms in a given cell determine the Tpm functions of that cell (Bakin et al., 2004; Lee et al., 2000; Varga et al., 2005; Wawro et al., 2007).

Several genes targeted by TGFβ, including *Tpm1*, *Tpm2*, and genes encoding α-actinin1 and calponin2-encoding actin-binding proteins, have been implicated in the assembly of stress fibers (Bakin et al., 2004; Zheng et al., 2008). Of these, Tpms have been shown to play a crucial role in stabilizing actin filaments (Pawlak and Helfman, 2001). TGFβ specifically upregulates the expression of *Tpm1* and *Tpm2*, but does not regulate the expression of *Tpm3* or *Tpm4*, which encode low-molecular-weight Tpms (Bakin et al., 2004; Zheng et al., 2008). Evaluation of the expression of Tpm1 and Tpm2 in MLECs and human LECs showed that the growth and differentiation of LECs are differentially regulated by TGFβ and fibroblast growth factor 2 (FGF2) (Kubo et al., 2017). TGFβ was found to induce epithelial to myofibroblastic transition (EMyoT) and expression of Tpm1, Tpm2 and α-SMA, whereas FGF2 suppressed the TGFβ2-induced up-regulation of these mRNAs and proteins. Depletion of Tpm1 and Tpm2 by siRNA and FGF2 addition suppressed the formation of stress fibers and activated fibroblastic LECs, which lost cell polarity inducing their migration (Kubo et al., 2017).

The present study was designed to evaluate the role of Tpm2 in mouse lens morphology, wound healing and cell migration by generating *Tpm2* heterozygous knockout (*Tpm2*$^{+/-}$) mice. The study showed that mouse lenses deficient in Tpm2 resulted in the inhibition of EMT during wound healing of LECs, as well as causing lens opacity. In addition, our results indicate that low levels of Tpm2 in the lenses may contribute to cataract formation.

2. Materials and methods

2.1. Animals

All animal experiments were approved by the Committee of Animal Research at the Kanazawa Medical University and conducted in accordance with the National Institutes of Health Guide for the Care and Use of Laboratory Animals, the Association for Research in Vision and Ophthalmology (ARVO) Statement on the Use of Animals in Ophthalmic and

Vision Research, and the Institutional Guidelines for laboratory animals (Permission number: 2016–35) and recombinant DNA experiments (Permission number: 2015–11) of Kanazawa Medical University. C57BL/6J mice were purchased from Sankyo Laboratories Japan (Ishikawa, Japan).

2.2. Surgical procedure

Twelve eyes of six 7-week-old, female C57BL/6J wild type (*Tpm2*$^{+/+}$) mice were used as a mouse model of PCO. Extra capsular lens extraction (ECLE) was performed in all eyes using a procedure previously described (Kubo et al., 2013). Briefly, mice were anesthetized by intraperitoneal administration of combination anesthetic containing 0.3 mg/kg medetomidine, 4.0 mg/kg midazolam, and 5.0 mg/kg butorphanol (WAKO, Osaka, Japan). The surgery was performed by first making a corneal incision with a keratome (Alcon Japan Ltd., Tokyo, Japan). Capsulorrhexis was performed with a marking straight knife (MANI®, Utsunomiya, Japan) followed by lens removal. At day 7 after surgery, the animals were sacrificed by administration of a lethal dose of CO_2. Real-time reverse transcriptase-PCR (RT-PCR) was used in all eyes to confirm whether *Tpm2* mRNA expression was elevated.

2.3. Vector construction

The activity of gene-targeted endonucleases was determined by Cel-I nuclease digestion of the PCR-amplified targeted region and/or the single strand annealing (SSA) assay, which reconstitutes reporter gene expression using a pCAG-EGxxFP plasmid containing 5′ and 3′ EGFP fragments that share 482 bp under the control of a ubiquitous CAG promoter (Fujihara and Ikawa, 2014; Mashiko et al., 2013; Okabe et al., 1997). The clustered regularly interspaced short palindromic repeat/ Cas9 (CRISPR/Cas9) expression vector construction has been described (Mizuno et al., 2014; Okabe et al., 1997). Briefly, oligo-DNAs (5′-caccggagaatgccatcgaccgcg-3′ and 5′-aaaccgcggtcgatggcattctcc –3′) were annealed and then purified by ethanol precipitation. The double stranded DNA was inserted into the BbsI restriction site in the px330 vector (Addgene, Cambridge, MA, USA) using enzyme KOD/FX (Toyobo Osaka Japan). The plasmid was designated px330-Tpm2 as a target of all 4 Tpm2 isoforms.

2.4. Microinjection

Unfertilized eggs of C57BL/6NCr mice were collected from the oviduct. Then, 5 ng/ul of Px330-Tpm DNA vector (circular) was injected into the pronuclei of these one-cell-stage embryos according to standard protocols (Gordon and Ruddle, 1981). The injected one-cell embryos were then transferred into pseudopregnant C57BL/6NCr mice. After 19 days, offspring were acquired by natural birth or Caesarean section, and were analyzed utilizing direct sequence analysis Applied Biosystems® 3130xI Genetic Analyzer (Thermo Fisher Scientific Japan Ltd., Tokyo, Japan) at about 1-week-old.

2.5. Genomic PCR and sequence analysis

Founder mice were screened, and off-target effects were examined by PCR and direct sequencing using DNA obtained from the tail. PCR was performed using enzyme Taq DNA Polymerase (Feldan, DOT Scientific, Inc., Burton, MI, USA) with a TaKaRa PCR Thermal

Cycler Dice® Gradient (Tokyo, Japan) and primers 5′-gtgcttctgcccctacaagg-3′ (forward) and 5′-tagtgttagaaggccctggg-3′ (reverse). Products were sequenced by Applied Biosystems® 3500xL (Thermo Fisher Scientific Japan Ltd.) to verify the presence of mutations.

2.6. Real-time RT-PCR

Total RNA was extracted from mouse liver and heart using TRIZOL reagent (Invitrogen™, ThermoFisher Scientific Japan Ltd.) according to the manufacturer's instructions. Total RNA was extracted from mouse LECs and lens cortex using RNeasy Mini Kits (Qiagen, Valencia, CA, USA) as described by the manufacturer. The relative expressions of mouse *Tpm1*, *Tpm2*, and *αSMA* mRNAs were determined using Prism7300 (Applied Biosystems®). Sequences were PCR amplified using TaqMan Universal Master Mix and; a pre-developed mouse Tpm2 probe mix (Assay ID: Mm00437172_g1) (Applied Biosystems®), which recognizes the transcript variants of Tpm2.1, 2.2, and 2.3 isoforms; a pre-developed mouse Tpm1 probe mix (Assay ID: Mm00445895_g1), which recognizes the transcript variant of Tpm1.1, 1.2, 1.6, 1.8, 1.10, 1.12; and 1.13, or a pre-developed mouse *αSMA* probe mix (Assay ID: Mm00725412_s1). The relative expression levels of *Tpm1*, *Tpm2* and *αSMA* mRNA were determined using the comparative Ct method and normalized relative to a pre-developed TaqMan ribosomal RNA control reagent VIC probe as an endogenous control (Applied Biosystems®).

2.7. Microscopic, histological and immunohistochemical analyses

Retroillumination images of lenses of 53-week-old mice were photographed using a Casey eye institute (CEI) camera system (Fraunfelder et al., 2011). Briefly, mouse eyes were fixed for 48 h in 10% neutral buffered formalin, embedded in paraffin and sectioned at approximately 4 μm. Eyes were immunostained using a Tyramide Signal Amplification (TSA™) Kit (Molecular Probes Inc., ThermoFisher Scientific Japan Ltd.), following the manufacturer's protocol and as described (Kubo et al., 2013; Kubo et al., 2006). Tpm1 and Tpm2 were visualized using anti-mouse Tpm (TM311) monoclonal antibody (Ab) (abcam Inc., Cambridge, MA, USA), which recognizes Tpm1 (39 kDa) and Tpm2 (36 kDa) isoforms; anti-mouse F-actin Ab (abcam Inc.); and anti-mouse αSMA monoclonal Ab (Sigma, St. Louis, MO, USA). Cell nuclei were stained with 4′,6-diamidino-2-phenylindole (DAPI) (Fluoroshield Mounting Medium with DAPI: ImmunoBioScience Corp., Mukilteo, WA). For negative controls (NC), mouse IgG isotype control (Dako, Agilent, Santa Clara, CA) was used and the primary antibody was omitted. NC were performed in parallel to all experiments.

2.8. In vivo wound healing assay

The PCO wound healing model was generated in 7-week-old mice as described, with modifications (Tanaka et al., 2010). Briefly, six $Tpm2^{+/-}$ and six $Tpm2^{+/+}$ mice were anesthetized by intraperitoneal injection of a combination of 0.3 mg/kg medetomidine, 4.0 mg/kg midazolam, and 5.0 mg/kg butorphanol (WAKO) (Tanaka et al., 2010). Following topical application of mydriatics, the central anterior lens capsule was pierced once with the blade of a 31 gauge needle, to a depth of about 2.5 mm from the corneal surface. Eyes without punctured lenses were examined as negative controls (non-injured). After instillation

of 0.3% ofloxacin ointment (Nitto Medic Co., Ltd., Toyama, Japan), the mice were allowed to heal for 5 and 10 days. The enucleated eye globes were fixed and embedded in paraffin for histological and immunohistochemical examinations.

2.9. Statistical analysis

Each experiment was performed in triplicate and repeated at least three times. Data were reported as mean ± standard deviation (SD) and analyzed by one-way ANOVA with post-hoc Tukey HSD. All statistical analyses were performed using StatMate2.0 (GraphPad Software, Inc. La Jolla, CA, USA), with P-values less than 0.05 considered statistically significant.

3. Results

3.1. Altered expression of Tpm 2 mRNA in LECs of a mouse model of PCO

We previously reported that the expression of *Tpm2* mRNA and protein was elevated in a rat model of PCO (Kubo et al., 2013). To determine whether *Tpm2* mRNA and *αSMA* mRNA as EMT markers were also elevated in a mouse model of PCO, we assayed *Tpm2* mRNA by real time PCR in mouse lens epithelia after ECLE. On day 7, expression of *Tpm2* and *αSMA* mRNA was highly elevated (*$p < 0.002$) (Fig. 1), similar to findings in the rat PCO model (Kubo et al., 2013) showing that Tpm2 and EMT are involved in the progression of PCO in mice.

3.2. Expression levels of Tpm2, Tpm1, and αSMA mRNAs in lens, cardiac muscle and liver of Tpm2$^{+/-}$ and Tpm2$^{+/+}$ mice

Because the expression of Tpm2 protein was extremely low in the eye lenses of both *Tpm2*$^{+/-}$ and *Tpm2*$^{+/+}$ mice, it was necessary to determine whether expression of *Tpm2* mRNA is reduced in *Tpm2*$^{+/-}$ mice by real time PCR assays in lens, cardiac muscle and liver tissues. We found that the levels of *Tpm2* mRNA in liver and heart were significantly lower in *Tpm2*$^{+/-}$ than in *Tpm2*$^{+/+}$ mice (*$p < 0.05$) (Fig. 2A and B). In contrast, the levels of *Tpm1* and *αSMA* mRNAs in the lens did not differ significantly between *Tpm2*$^{+/-}$ and *Tpm2*$^{+/+}$ mice (Fig. 2C).

3.3. Microscopic and histological changes in aging lenses of Tpm2$^{+/-}$ mice

No histological changes were observed in normal lenses of 7-week-old *Tpm2*$^{+/-}$ mice (Data not shown). Small vacuoles and slight swelling of lens fiber were observed in 16-week-old *Tpm2*$^{+/-}$ (Fig. 3A-b) but not *Tpm2*$^{+/+}$ (Fig. 3A-a) mice. Retroillumination images of lenses of 53-week-old *Tpm2*$^{+/-}$ mice showed central opacity in the anterior cortex under the LECs (Fig. 3B-c). Histological observation revealed the disorganization of fibers and formation of vacuoles at the lens anterior surface (Fig. 3B-d). In contrast, microscopic examination revealed that slight opacity was observed in lenses of 53-week old *Tpm2*$^{+/+}$ mice (Fig. 3B-a). Further, small vacuoles under the lens capsule were observed in lenses of 53-week old *Tpm2*$^{+/+}$ mice (Fig. 3B-b). The anterior and equatorial-bow regions of lenses in 86-week-old *Tpm2*$^{+/-}$ mice showed progression of swelling, liquefaction and fiber disruption (Fig. 3C-c and –d). Lenses of 86-week-old *Tpm2*$^{+/+}$ mice also showed formation of small vacuoles, but to a much lesser extent than in *Tpm2*$^{+/-}$ mice (Fig. 3C-a and –b). Further,

immunolocalization of F-actin was lower in lenses of 53-week-old *Tpm2*$^{+/-}$ than 53-week-old *Tpm2*$^{+/+}$ mice (Fig. 3D-a and –b)

3.4. Effect of Tpm2 knock-down on wound healing of lens surface in vivo

Wounded areas showed fibroblast-like tissue changes, indicating EMT. On days 5 and 10 after needle puncture, fibroblastic changes around the wounded area were smaller in *Tpm2*$^{+/-}$ than in *Tpm2*$^{+/+}$ mice (Fig. 4A-a, –c and B-a, –c). No morphological changes were observed in lenses from non-injured controls (Fig. 4A-b, –d and B-b, –d). Immunofluorescence staining also showed that Tpm1 and Tpm2 positive areas were smaller in lenses of *Tpm2*$^{+/-}$ than *Tpm2*$^{+/+}$ mice on days 5 and 10 (Fig. 5A-a, –b and B-a, –b). Fibroblastic LECs at the wound surface were immunopositive for αSMA on days 5 and 10 in both *Tpm2*$^{+/+}$ and *Tpm2*$^{+/-}$ mice. The intensity of staining for αSMA close to the wounded site in *Tpm2*$^{+/-}$ mice was less comparing to in *Tpm2*$^{+/+}$ mice (Fig. 5A-e, –f and B-e, –f). Negative control (NC) lenses from *Tpm2*$^{+/+}$ and *Tpm2*$^{+/-}$ mice with/without injury showed no evidence of specific immunostaining (Fig. 5A–i, –j, –k, –l and B–i, –j, –k, –l). There was no positive staining for Tpm2 or αSMA in non-injured controls (Fig. 5A-c, –d, –g, –h and B-c, –d, –g, –h). Nuclear counter stain was performed using DAPI (Fig. 5m, –n, –o, –p and B-m, –n, –o, –p)

4. Discussion

This study was designed to evaluate the physiological role of Tpm2 in the pathogenesis of cataract by generating a line of *Tpm2*$^{+/-}$ mice. CRISPR/Cas-mediated genome editing generated a global *Tpm2* mutation in ES cells. Homozygous loss of *Tpm2* resulted in embryonic lethality in mice suggesting *Tpm2* is essential for development and life. Previous knockout mouse models have also shown that Tpm genes are essential for life, as deletion of Tpm1, 2, and 3 genes was embryonically lethal (Blanchard et al., 1997; Hook et al., 2004; Hook et al., 2011; Jagatheesan et al., 2010; Rethinasamy et al., 1998; Schevzov et al., 2011). Therefore, the role of Tpm2 in the lens was analyzed using *Tpm2*$^{+/-}$ mice, a model characterized by reduced expression of *Tpm2* in the lens, as well as the liver and cardiac muscle. Interestingly, *Tpm2*$^{+/-}$did not affect the expression of Tpm1 or αSMA, both of which are involved in EMT. Therefore, it is likely that the phenotype displayed in this animal model is mostly, if not solely, due to *Tpm2* gene deletion.

Tpm2$^{+/-}$ mice showed earlier onset and faster progression of cataract during aging than did age-matched *Tpm2*$^{+/+}$ mice. Opacity in *Tpm2*$^{+/-}$ mice appeared first in the cortical zone at the center of the lens and gradually spread into the equatorial to bow region becoming more noticeable at age 16-weeks. Older mice showed progressive lens opacity, along with swelling and liquefaction of lens fibers in the equatorial to bow region, increasing with age up to age 86-weeks. Although older (> 53 weeks) *Tpm2*$^{+/+}$ mice showed histological changes, such as vacuoles in surface lens fibers, these changes were slight compared to the marked pathological changes of lens fibers in the cortical region in *Tpm2*$^{+/-}$mice. These findings indicate that *Tpm2*$^{+/-}$may induce lens opacity and disrupt the differentiation of lens fibers in the cortical region. Thus, Tpm2 may play a role in the differentiation of newly formed lens fibers. Tpms contribute to the spatial and temporal regulation of the actin

cytoskeleton in an isoform-specific manner, by regulating the association of actin with various actin-binding proteins including F-actin (Gunning et al., 2008; Gunning et al., 2015). In this study, we found expression of F-actin was decreased in 53-week-old mouse lenses. Tpms have been shown to stabilize actin filaments and bind to F-actin (Gateva et al., 2017; Pawlak and Helfman, 2001). *Tpm2*$^{+/-}$ may suppress the stabilization of actin filament inducing the formation of unstable F-actin. Although expression of Tpm2 is very low in mouse lenses, this protein may be necessary to maintain the actin cytoskeleton of lens fiber, and lens fiber arrangement and shape.

This study also showed that fibroblastic, EMT-like changes in a model of mouse lens injury were less severe in *Tpm2*$^{+/-}$ than in *Tpm2*$^{+/+}$ mice, suggesting depletion of *Tpm2* may delay wound healing in mouse lenses and that Tpm2 may play a critical role in the induction of EMT in lenses. Further, expression of αSMA was reduced in the injured area of *Tpm2*$^{+/-}$ mice. Tpms contribute to the spatial and temporal regulation of the actin cytoskeleton in an isoform-specific manner, by regulating the association of actin with various actin-binding proteins (Gunning et al., 2008; Gunning et al., 2015; Jalilian et al., 2015). We found that *Tpm1* and *Tpm2* knock-down by siRNAs inhibited TGFβ2-induced formation of stress fibers (Kubo et al., 2017), suggesting that Tpms may induce stress fibers in response to TGFβ2 during the EMT process.

We previously reported that MLECs deficient in Prdx6 showed phenotypic changes characteristic of terminal cell differentiation and EMT (Kubo et al., 2010). Prdx6 provides cytoprotection against internal and external environmental stressors and plays a role in cellular signaling by detoxifying ROS, thereby regulating gene expression (Kubo et al., 2008; Kubo et al., 2010; Manevich and Fisher, 2005; Wood et al., 2003). Proteomic analysis showed that the expressions of Tpm1 and Tpm2 were elevated in *Prdx6*$^{-/-}$LECs, with exogenous Prdx6 reducing Tpm2 expression (Kubo et al., 2010). The expression of *Tpm2* mRNA was extremely lower than that of *Tpm1* mRNA in the eye lenses, however the expression of Tpm2 in *Prdx6*$^{-/-}$ LECs was surprisingly high compared to that in wild type LECs (*Prdx6*$^{+/+}$ > 120-fold higher). We therefore hypothesized that, because Tpms have been implicated in the regulation of cellular activities by stabilizing ECM proteins (specifically actin microfilaments), aberrant expression of Tpm2 is likely involved in phenotypic alterations in *Prdx6*$^{-/-}$ MLECs. From this reasoning, we first selected *Tpm2* for knockout experiments rather than *Tpm1*. Now, we are studying the effects of *Tpm1* deficiency using *Tpm1* conditional knockout mice in eye lenses. Moreover, the expressions of Tpm1 and Tpm2 in an *in vivo* rat model of PCO was increased during EMT, with selective elevation of Tpm1 and Tpm2 in rat LECs correlating with fibrosis (Kubo et al., 2013). The elevated expression of Tpm1 and Tpm2 resulted in the transdifferentiation of LECs into multilayered, spindle-shaped LECs in a rat model of PCO, in human eyes with anterior sub-capsular cataract, and in human differentiated LECs in a dislocated lens capsule (Kubo et al., 2013). These findings suggested that the expressions of Tpm1 and Tpm2 may be associated with the progression of PCO (Kubo et al., 2013). In normal mouse lenses, the expression of Tpm2 protein is very low and cannot be detected. However, following induction of PCO by ECLE, the expression of Tpm2 was highly increased, suggesting that increased expression of Tpm2 may induce EMT and PCO and that knock-down of the *Tpm2* gene may inhibit EMT and PCO.

In summary, this study showed that Tpm2 may be important in maintaining lens physiology and morphology. Upregulation of Tpm2 may be involved in the progression of EMT in mouse PCO and wound healing in mice LECs. Thus, inhibition of Tpm2 may reduce EMT changes in PCO or wound healing in lenses. Tpm2 may represent an important biomarker and a therapeutic target in the treatment of PCO and wound healing linked to EMT and tissue fibrosis.

Acknowledgments

This work was supported by grants from Japan Society for the Promotion of Science (JSPS) KAKENHI Grant Numbers JP23592588 (to Eri Kubo), National Eye Institute, National Institute of Health (NIH) (EY024589) (to DPS) and Research for Preventing Blindness (to DPS). Their support is gratefully acknowledged.

Abbreviations

EMT	mesenchymal transition
PCO	posterior capsular opacification
CRISPR/Cas9	clustered regularly interspaced short palindromic repeat/Cas9
LECs	lens epithelial cells
Nd	YAG, neodymium-doped yttrium aluminum garnet
Tpm	tropomyosin
ROS	reactive oxygen species
TGF	transforming growth factor
αSMA	α smooth muscle actin
Prdx6	peroxiredoxin 6
Prdx6$^{-/-}$	Prdx6-deficient
MLECs	mouse LECs
ECM	extracellular matrix
FGF2	fibroblast growth factor 2
EMyoT	epithelial to myofibroblastic transition
***Tpm2*$^{+/-}$**	*Tpm2* heterozygous knockout
ARVO	Association for Research in Vision and Ophthalmology
***Tpm2*$^{+/+}$**	wild type
ECLE	extra capsular lens extraction
RT-PCR	reverse transcriptase-PCR

SSA	single strand annealing
CEI	Casey eye institute
Ab	antibody
DAPI	4′,6-diamidino-2-phenylindole
NC	negative controls
SD	standard deviation

References

Apple DJ, Solomon KD, Tetz MR, Assia EI, Holland EY, Legler UF, Tsai JC, Castaneda VE, Hoggatt JP, Kostick AM. Posterior capsule opacification. Surv Ophthalmol. 1992; 37:73–116. [PubMed: 1455302]

Awasthi N, Guo S, Wagner BJ. Posterior capsular opacification: a problem reduced but not yet eradicated. Arch Ophthalmol. 2009; 127:555–562. [PubMed: 19365040]

Bakin AV, Safina A, Rinehart C, Daroqui C, Darbary H, Helfman DM. A critical role of tropomyosins in TGF-beta regulation of the actin cytoskeleton and cell motility in epithelial cells. Mol Biol Cell. 2004; 15:4682–4694. [PubMed: 15317845]

Blanchard EM, Iizuka K, Christe M, Conner DA, Geisterfer-Lowrance A, Schoen FJ, Maughan DW, Seidman CE, Seidman JG. Targeted ablation of the murine alpha-tropomyosin gene. Circ Res. 1997; 81:1005–1010. [PubMed: 9400381]

de Iongh RU, Wederell E, Lovicu FJ, McAvoy JW. Transforming growth factor-beta-induced epithelial-mesenchymal transition in the lens: a model for cataract formation. Cells Tissues Organs. 2005; 179:43–55. [PubMed: 15942192]

Fatma N, Kubo E, Sharma P, Beier DR, Singh DP. Impaired homeostasis and phenotypic abnormalities in Prdx6−/−mice lens epithelial cells by reactive oxygen species: increased expression and activation of TGFbeta. Cell Death Differ. 2005; 12:734–750. [PubMed: 15818411]

Fatma N, Kubo E, Sen M, Agarwal N, Thoreson WB, Camras CB, Singh DP. Peroxiredoxin 6 delivery attenuates TNF-alpha-and glutamate-induced retinal ganglion cell death by limiting ROS levels and maintaining Ca2+ homeostasis. Brain Res. 2008; 1233:63–78. [PubMed: 18694738]

Fraunfelder FT, Steinkamp P, Fraunfelder FW. Casey Eye Institute camera system for recording lens opacities. Exp Eye Res. 2011; 93:790–794. [PubMed: 21958933]

Fujihara Y, Ikawa M. CRISPR/Cas9-based genome editing in mice by single plasmid injection. Methods Enzymol. 2014; 546:319–336. [PubMed: 25398347]

Gateva G, Kremneva E, Reindl T, Kotila T, Kogan K, Gressin L, Gunning PW, Manstein DJ, Michelot A, Lappalainen P. Tropomyosin isoforms specify functionally distinct actin filament populations *in vitro*. Curr Biol. 2017; 27:705–713. [PubMed: 28216317]

Geeves MA, Hitchcock-DeGregori SE, Gunning PW. A systematic nomenclature for mammalian tropomyosin isoforms. J Muscle Res Cell Motil. 2015; 36:147–153. [PubMed: 25369766]

Gordon JW, Ruddle FH. Integration and stable germ line transmission of genes injected into mouse pronuclei. Science. 1981; 214:1244–1246. [PubMed: 6272397]

Gunning PW, Schevzov G, Kee AJ, Hardeman EC. Tropomyosin isoforms: divining rods for actin cytoskeleton function. Trends Cell Biol. 2005; 15:333–341. [PubMed: 15953552]

Gunning P, O'Neill G, Hardeman E. Tropomyosin-based regulation of the actin cytoskeleton in time and space. Physiol Rev. 2008; 88:1–35. [PubMed: 18195081]

Gunning PW, Hardeman EC, Lappalainen P, Mulvihill DP. Tropomyosin –master regulator of actin filament function in the cytoskeleton. J Cell Sci. 2015; 128:2965–2974. [PubMed: 26240174]

Hook J, Lemckert F, Qin H, Schevzov G, Gunning P. Gamma tropomyosin gene products are required for embryonic development. Mol Cell Biol. 2004; 24:2318–2323. [PubMed: 14993271]

Hook J, Lemckert F, Schevzov G, Fath T, Gunning P. Functional identity of the gamma tropomyosin gene: implications for embryonic development, reproduction and cell viability. Bioarchitecture. 2011; 1:49–59. [PubMed: 21866263]

Jagatheesan G, Rajan S, Wieczorek DF. Investigations into tropomyosin function using mouse models. J Mol Cell Cardiol. 2010; 48:893–898. [PubMed: 19835881]

Jalilian I, Heu C, Cheng H, Freittag H, Desouza M, Stehn JR, Bryce NS, Whan RM, Hardeman EC, Fath T, Schevzov G, Gunning PW. Cell elasticity is regulated by the tropomyosin isoform composition of the actin cytoskeleton. PLoS One. 2015; 10:e0126214. [PubMed: 25978408]

Kubo E, Miyazawa T, Fatma N, Akagi Y, Singh DP. Development- and age-associated expression pattern of peroxiredoxin 6, and its regulation in murine ocular lens. Mech Ageing Dev. 2006; 127:249–256. [PubMed: 16321424]

Kubo E, Fatma N, Akagi Y, Beier DR, Singh SP, Singh DP. TAT-mediated PRDX6 protein transduction protects against eye lens epithelial cell death and delays lens opacity. Am J Physiol Cell Physiol. 2008; 294:C842–855. [PubMed: 18184874]

Kubo E, Hasanova N, Tanaka Y, Fatma N, Takamura Y, Singh DP, Akagi Y. Protein expression profiling of lens epithelial cells from Prdx6-depleted mice and their vulnerability to UV radiation exposure. Am J Physiol Cell Physiol. 2010; 298:342–354.

Kubo E, Hasanova N, Fatma N, Sasaki H, Singh DP. Elevated tropomyosin expression is associated with epithelial-mesenchymal transition of lens epithelial cells. J Cell Mol Med. 2013; 17:212–221. [PubMed: 23205574]

Kubo E, Shibata S, Shibata T, Kiyokawa E, Sasaki H, Singh DP. FGF2 antagonizes aberrant TGFbeta regulation of tropomyosin: role for posterior capsule opacity. J Cell Mol Med. 2017; 21:916–928. [PubMed: 27976512]

Lee A, Fischer RS, Fowler VM. Stabilization and remodeling of the membrane skeleton during lens fiber cell differentiation and maturation. Dev Dyn. 2000; 217:257–270. [PubMed: 10741420]

Liu RM, Gaston Pravia KA. Oxidative stress and glutathione in TGF-beta-mediated fibrogenesis. Free Radic Biol Med. 2010; 48:1–15. [PubMed: 19800967]

Lovicu FJ, McAvoy JW. Structural analysis of lens epithelial explants induced to differentiate into fibres by fibroblast growth factor (FGF). Exp Eye Res. 1989; 49:479–494. [PubMed: 2792239]

Manevich Y, Fisher AB. Peroxiredoxin 6, a 1-Cys peroxiredoxin, functions in antioxidant defense and lung phospholipid metabolism. Free Radic Biol Med. 2005; 38:1422–1432. [PubMed: 15890616]

Marcantonio JM, Syam PP, Liu CS, Duncan G. Epithelial transdifferentiation and cataract in the human lens. Exp Eye Res. 2003; 77:339–346. [PubMed: 12907166]

Mashiko D, Fujihara Y, Satouh Y, Miyata H, Isotani A, Ikawa M. Generation of mutant mice by pronuclear injection of circular plasmid expressing Cas9 and single guided RNA. Sci Rep. 2013; 3:3355. [PubMed: 24284873]

McAvoy JW, Chamberlain CG, de Iongh RU, Hales AM, Lovicu FJ. Peter Bishop lecture: growth factors in lens development and cataract: key roles for fibroblast growth factor and TGF-beta. Clin Exp Ophthalmol. 2000; 28:133–139. [PubMed: 10981780]

McDonnell PJ, Rowen SL, Glaser BM, Sato M. Posterior capsule opacification. An in vitro model Arch Ophthalmol. 1985; 103:1378–1381. [PubMed: 4038131]

Meacock WR, Spalton DJ, Stanford MR. Role of cytokines in the pathogenesis of posterior capsule opacification. Br J Ophthalmol. 2000; 84:332–336. [PubMed: 10684849]

Mizuno S, Dinh TT, Kato K, Mizuno-Iijima S, Tanimoto Y, Daitoku Y, Hoshino Y, Ikawa M, Takahashi S, Sugiyama F, Yagami K. Simple generation of albino C57BL/6J mice with G291T mutation in the tyrosinase gene by the CRISPR/Cas9 system. Mamm Genome. 2014; 25:327–334. [PubMed: 24879364]

Okabe M, Ikawa M, Kominami K, Nakanishi T, Nishimune Y. 'Green mice' as a source of ubiquitous green cells. FEBS Lett. 1997; 407:313–319. [PubMed: 9175875]

Pawlak G, Helfman DM. Cytoskeletal changes in cell transformation and tumorigenesis. Curr Opin Genet Dev. 2001; 11:41–47. [PubMed: 11163149]

Rethinasamy P, Muthuchamy M, Hewett T, Boivin G, Wolska BM, Evans C, Solaro RJ, Wieczorek DF. Molecular and physiological effects of alpha-tropomyosin ablation in the mouse. Circ Res. 1998; 82:116–123. [PubMed: 9440710]

Rungger-Brandle E, Conti A, Leuenberger PM, Rungger D. Expression of alphasmooth muscle actin in lens epithelia from human donors and cataract patients. Exp Eye Res. 2005; 81:539–550. [PubMed: 15935344]

Saika S. Relationship between posterior capsule opacification and intraocular lens biocompatibility. Prog Retin Eye Res. 2004; 23:283–305. [PubMed: 15177204]

Schevzov G, Whittaker SP, Fath T, Lin JJ, Gunning PW. Tropomyosin isoforms and reagents. Bioarchitecture. 2011; 1:135–164. [PubMed: 22069507]

Tanaka S, Sumioka T, Fujita N, Kitano A, Okada Y, Yamanaka O, Flanders KC, Miyajima M, Saika S. Suppression of injury-induced epithelial-mesenchymal transition in a mouse lens epithelium lacking tenascin-C. Mol Vis. 2010; 16:1194–1205. [PubMed: 20664686]

Thiery JP. Epithelial-mesenchymal transitions in development and pathologies. Curr Opin Cell Biol. 2003; 15:740–746. [PubMed: 14644200]

Tripathi BJ, Tripathi RC, Livingston AM, Borisuth NS. The role of growth factors in the embryogenesis and differentiation of the eye. Am J Anat. 1991; 192:442–471. [PubMed: 1781453]

Varga AE, Stourman NV, Zheng Q, Safina AF, Quan L, Li X, Sossey-Alaoui K, Bakin AV. Silencing of the Tropomyosin-1 gene by DNA methylation alters tumor suppressor function of TGF-beta. Oncogene. 2005; 24:5043–5052. [PubMed: 15897890]

Vindin H, Gunning P. Cytoskeletal tropomyosins: choreographers of actin filament functional diversity. J Muscle Res Cell Motil. 2013; 34:261–274. [PubMed: 23904035]

Wawro B, Greenfield NJ, Wear MA, Cooper JA, Higgs HN, Hitchcock-DeGregori SE. Tropomyosin regulates elongation by formin at the fast-growing end of the actin filament. Biochemistry. 2007; 46:8146–8155. [PubMed: 17569543]

Wood ZA, Schroder E, Robin Harris J, Poole LB. Structure, mechanism and regulation of peroxiredoxins. Trends Biochem Sci. 2003; 28:32–40. [PubMed: 12517450]

Wormstone IM. Posterior capsule opacification: a cell biological perspective. Exp Eye Res. 2002; 74:337–347. [PubMed: 12014915]

Zheng Q, Safina A, Bakin AV. Role of high-molecular weight tropomyosins in TGF-beta-mediated control of cell motility. Int J Cancer. 2008; 122:78–90. [PubMed: 17721995]

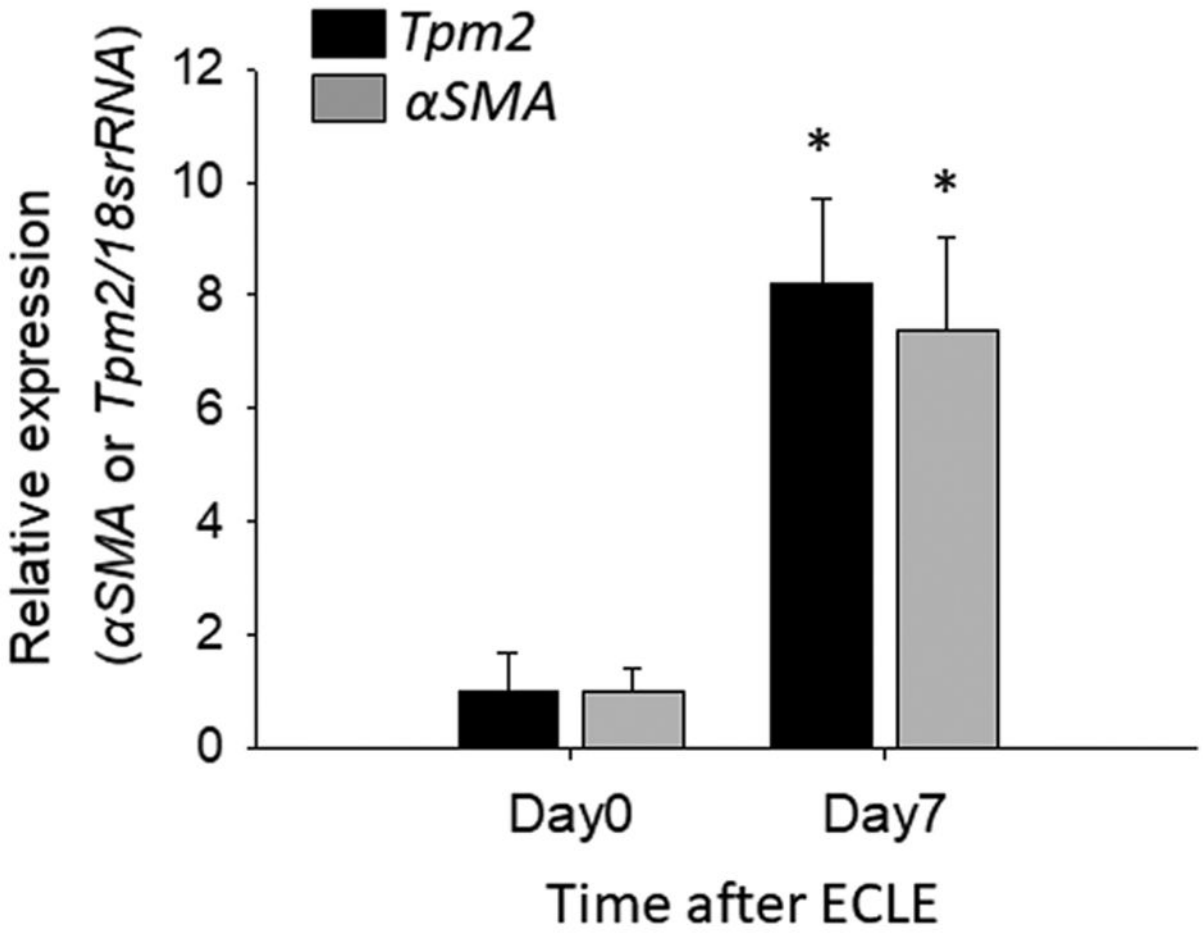

Fig. 1.

Upregulation of *Tpm2* and *αSMA* mRNAs in lens epithelium of a mouse model of PCO. *Tpm2* and *αSMA* mRNAs were expressed in lens epithelia of $Tpm2^{+/+}$ mice, with expressions higher on day 7 than day 0 after ECLE. N = 6 eyes at each time point.

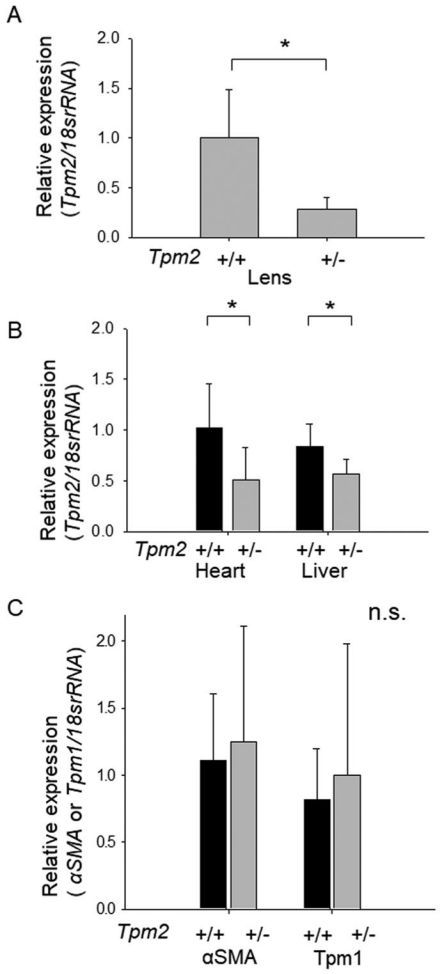

Fig. 2.

Downregulation of *Tpm2* mRNA in $Tpm2^{+/-}$ mice.

A: *Tpm2* mRNA levels and proteins measured by real-time RT-PCR and western blot were significantly lower in lens of $Tpm2^{+/-}$ than $Tpm2^{+/+}$ mice. Results represent the mean ± SD of three separate experiments. B: *Tpm2* mRNA measured by real-time RT-PCR was significantly lower in cardiac muscle and liver of $Tpm2^{+/-}$ than $Tpm2^{+/+}$ mice. Results represent the mean ± SD of three separate experiments.

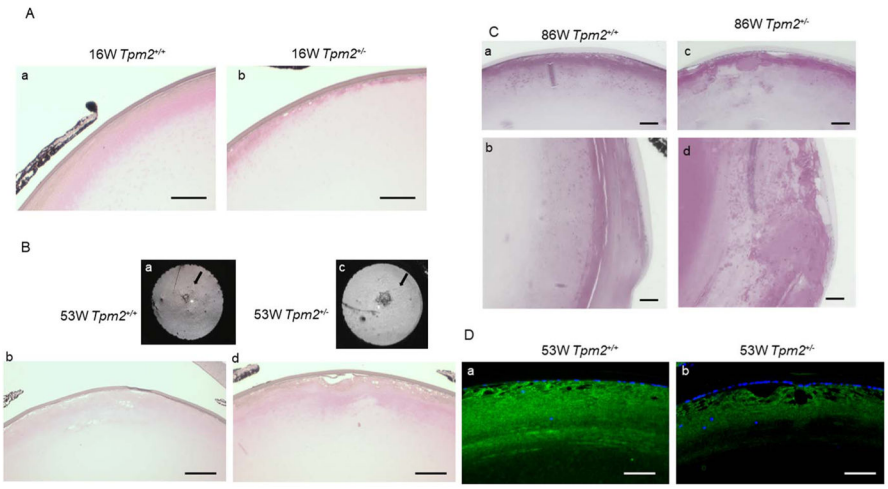

Fig. 3.

Histological changes and immunolocalization of F-actin in lenses of *Tpm2*$^{+/-}$ mice with aging.

Paraffin sections of lenses were prepared from mice aged 16, 53 and 86 weeks and stained with hematoxylin and eosin. Immunofluorescence staining was performed in lenses of 53-week-old, *Tpm2*$^{+/-}$ and *Tpm2*$^{+/+}$ mice using monoclonal anti-mouse F-actin Ab (A). Scale bar, 80 μm; n = 3.

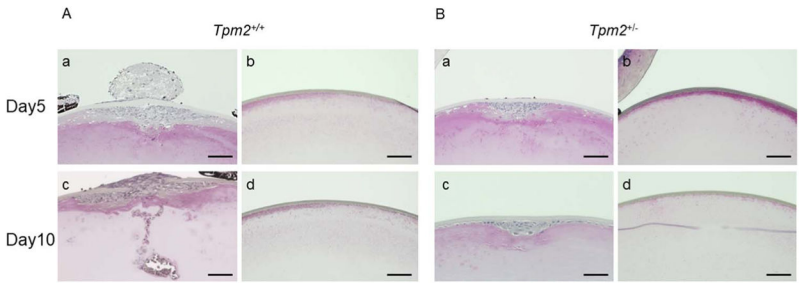

Fig. 4.

Tpm2$^{+/-}$ suppresses EMT and fibroblastic changes in injured mouse lenses.

Paraffin sections of lenses of *Tpm2*$^{+/-}$ and *Tpm2*$^{+/+}$ mice at 5 and 10 days with or without injury were prepared and stained with H & E. Scale bar, 200 μm. Results are representative of three independent experiments.

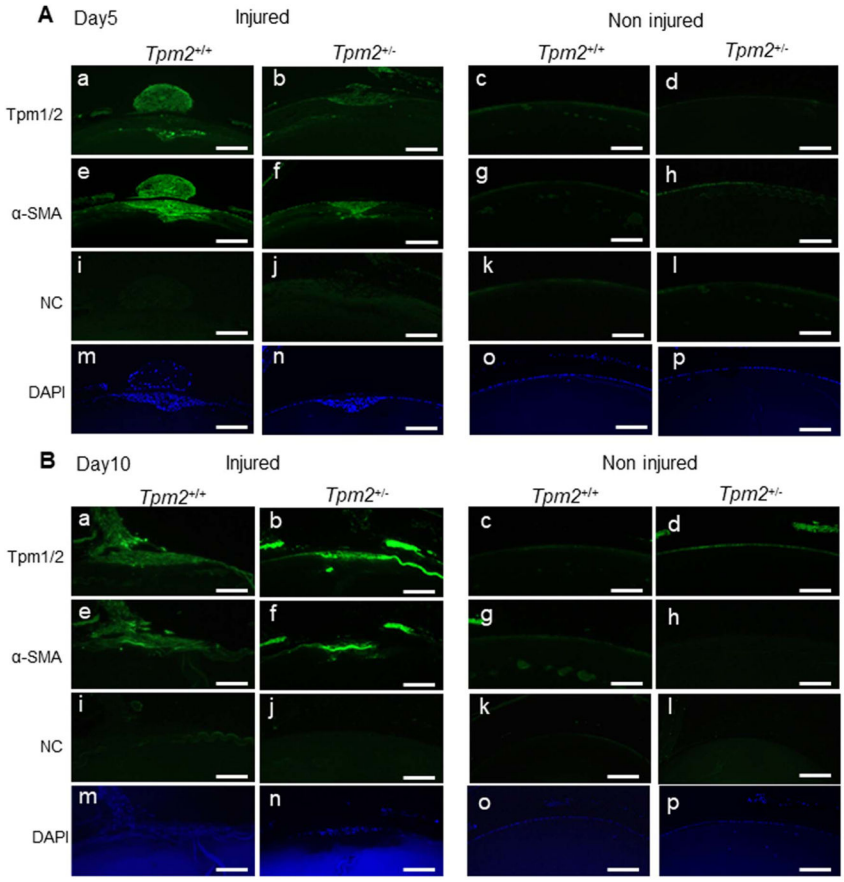

Fig. 5.

Tpm2$^{+/-}$ reduces immunolocalization of Tpm1 and Tpm2 and αSMA in injured mouse lenses.

Immunofluorescence staining was performed in lenses of *Tpm2*$^{+/-}$ and *Tpm2*$^{+/+}$ mice at 5 and 10 days after injury or no injury using monoclonal anti-mouse Tpm1 and Tpm2 Ab (A), which recognizes Tpm1 (39 kDa) and Tpm2 (36 kDa) isoforms, monoclonal anti-mouse αSMA Ab (B), anti-mouse IgG (NC) (C) and DAPI for nuclear counterstain (D). Scale bar, 200 μm. Results are representative of three independent experiments.